Impacts of Spatial Clustering of Urban Land Cover on Land Surface Temperature across Köppen Climate Zones in the Contiguous United States

Chuyuan Wang[1,*], Yubin Li[1], Soe W. Myint[1], Qunshan Zhao[2], Elizabeth A. Wentz[1]

[1] Spatial Analysis Research Center, School of Geographical Sciences and Urban Planning, Arizona State University, Tempe, AZ 85287, USA
[2] Urban Big Data Centre, School of Social and Political Sciences, University of Glasgow, Glasgow, G12 8RZ, UK
* Corresponding author; e-mail: chuyuanw@asu.edu

Highlights

- The effects of land covers' spatial clustering on LST are quantified using Moran's *I*.
- Seven metropolitan areas with different climate background in the U.S. are examined.
- Clustered impervious surfaces elevate LST except for Phoenix.
- The cooling effect of clustered green spaces was found in Phoenix and Portland only.
- Clustered water has a cooling effect during the daytime but a heating effect at night.

Impacts of Spatial Clustering of Urban Land Cover on Land Surface Temperature across Köppen Climate Zones in the Contiguous United States

Abstract

This study examines the effects of spatial clustering of urban land cover types on land surface temperature (LST). The potential impact of the background regional climate is also taken into consideration. To study this relationship, multiple cities, each representing a major Köppen climate region in the U.S., namely Portland, Los Angeles, Chicago, Denver, Kansas City, Orlando, and Phoenix, were selected. Urban land cover types were derived from the 2011 National Land Cover Database (NLCD); summer mean LST from 2011 was calculated using the Moderate Resolution Imaging Spectroradiometer (MODIS) LST products. Spatial clustering was quantified using Moran's *I*, and was analyzed against LST using correlation and multivariate regression analyses. The results indicate that in most climate regions, clustered impervious surfaces can elevate LST for both daytime and nighttime. The cooling effect of clustered vegetation cover was only found significant in regions with dry and warm summers, such as in Phoenix and Portland. Clustered water bodies have a strong cooling effect during the daytime but have a warming effect at night, except for cities such as Los Angeles and Phoenix, which have scant large water bodies. Furthermore, policy recommendations were put forward to suggest that reducing the spatial clustering of impervious surfaces, having more spatially clustered greenspaces, and having spatially dispersed water bodies with clustered greenspaces nearby are potential strategies to reduce urban warming in most cities in the contiguous U.S.

Keywords: spatial clustering; Moran's *I*; urban land cover; land surface temperature; Köppen climate classification

1. Introduction

Urbanization is the result of infrastructure development, built-up area expansion, and infilling driven by population growth. Currently, most of the human population resides in urban areas rather than rural areas (United Nations, 2018). This trend of increased urban living is projected to continue to 8.6 billion people projected by 2030, 9.8 billion by 2050, and 11.2 billion by 2100 (United Nations, 2009). With urban population growing at this magnitude, there is a critical need to understand how massive urban land use land cover (LULC) changes affect the local climate and environment (Carlson and Authur 2000; Lambin et al. 2001). It is well understood that urban land covers elevate land surface temperatures (LST) (Yue and Xu, 2013; Zhao et al., 2015; Wang et al., 2016; Chen et al., 2017; Tayyebi et al., 2018), which have a subsequent influence on the regional climate (Oke, 1982; Kalnay and Cai, 2003), plant phenology (Cleland et al. 2007; Karnieli et al. 2010), human health and comfort (Kalkstein and Smoyer, 1993; Kinney et al. 2001; Macintyre et al., 2018), and energy consumption and water use (Akbari et al. 2001; Guhathakurta and Gober, 2007; Kolokotroni et al. 2012). While mitigation strategies focus on reducing the area of impervious surfaces and increasing the amount of urban greenspaces, they lack details regarding the relative quantity and organization of these landscape features.

Research shows that spatial composition and configuration of land cover types have an influence on LST in urban environments. Spatial composition of the urban environment refers to the different land use categories, their total area, and the relative proportions (Gustafson, 1998). The empirical relationship between LULC composition and LST is well established across many cities around the world (Li et al., 2012; Song et al., 2014; Kuang et al., 2015; Nie et al., 2015; Estoque et al., 2017; Wang, et al., 2018; Zullo et al., 2018), such as a positive relationship between increased impervious surfaces and elevated LST and its inverse relationship with increased vegetation cover (Yuan and Bauer, 2007; Li, et al., 2012; Essa et al., 2013; Morabito et al., 2016; Wang et al., 2016). On the other hand, spatial configuration describes the spatial pattern of urban LULC patches in terms of shape, density, connectivity and complexity (Gustafson, 1998), which is normally quantified using landscape metrics. Many studies have examined the relationship between spatial configuration and LST for many cities around the world and have found a strong, positive relationship between density and connectivity of impervious surfaces and LST, and negative relationship with respect to vegetation cover (Zhang et al., 2009; Zhou et al., 2011; Li et al., 2012; Fan et al., 2014; Kong et al., 2014; Zheng et al., 2014; Zhou et al., 2014; Fan et al., 2015; Myint et al., 2015; Nie et al., 2015; Estoque et al., 2017; Gage et al., 2017; Nor et al., 2017; Masoudi et al., 2019). All of these have contributed to our understandings of how LULC influences LST and urban warming in terms of spatial composition and configuration.

What remains unknown about the relationship between land covers and LST is how spatial clustering of urban land cover types impacts LST and the effect of these relationships in different climate regions. Spatial clustering is different from the aforementioned spatial composition or configuration because it is a spatial structure quantity that measures how objects are spatially distributed and organized with certain dimensions (Cuzick and Edwards, 1990). Spatial clustering is often quantified using spatial autocorrelation indices, such as the widely used Moran's I (Moran, 1950), which indicates if objects are clustered, dispersed or randomly distributed in a given space. With the knowledge to reduce urban heat by reducing the area of impervious surfaces, growing cities are strained by the demands for roads, buildings, and urban structures. Instead of ad hoc, unplanned development, cities need to know how to plan for the organization of impervious surfaces combined with greenspaces. Furthermore, this needs to be done within the context of how a specific climate zone influences this relationship, building on research such as Zhao et al. (2014) who suggested that the local climate contributes to the urban heat island (UHI) effect. We therefore assert that the background climate may play an important role in influencing the relationship between the spatial clustering of land cover types and LST. We aim to build results on relationships between LST and land cover by exploring these relationships across varying background climate conditions using the Köppen climate system.

The Köppen climate classification system was developed by a German botanist-climatologist named Wladimir Köppen, who divided global climate into five major types, that is tropical, dry, temperate, continental, and polar climates. This system classifies climate groups based on mean temperature and precipitation (Kottek et al., 2006). In the contiguous United States, cities with a population of more than 100,000 are mostly located in dry, temperate, and continental climate regions. Researchers have been modeling and simulating urban climate change based on the Köppen climate classification (Bowler et al., 2010; Brown et al., 2015; Salata et al., 2015), but little has been done to systematically relate spatial clustering of urban land cover types and LST across different Köppen climate zones. The results can be potentially used to provide recommendations for policy makers and urban planners when planning for new constructions or urban renovation at a regional level.

This study has two objectives. First, to examine the empirical relationship between the spatial clustering of urban land cover types and LST in major cities in the contiguous U.S. using Moran's *I*. Second, to analyze the potential impacts of regional climate background of each city on the relationship.

2. Study Areas

We selected seven large metropolitan areas representing all the major climate regions in the Köppen classification system in the contiguous U.S., namely Portland, OR; Los Angeles, CA; Chicago, IL; Denver, CO; Kansas City, MO; Orlando, FL; and Phoenix, AZ. Phoenix and Denver have a dry climate (type "*B*"); Portland, Los Angeles, Kansas City, and Orlando have a temperate climate (type "*C*"), and Chicago has a continental climate (type "*D*"). These cities are representative of coastal (e.g. Los Angeles), inland (e.g. Kansas City), and lakeside (e.g. Chicago) regions with different climate backgrounds. They all have a metropolitan size larger than 1,000 km_2 and a population greater than 200,000 to ensure a large enough sample size for the subsequent statistical analyses. Selected cities and the Köppen climate classification of the contiguous U.S. are shown in Figure 1. Detailed information of each metropolitan area is summarized in Table 1.

Portland and Los Angeles have a Mediterranean climate with dry summer, which is denoted by "*Cs*" in the Köppen climate classification system. This climate is characterized by dry summers and cool, rainy winters. Although these two cities have the same major climate type, they are in different subcategories because Los Angeles has a monthly average temperature above 22 °C during summers, while Portland has an average temperature below 22 °C for all the 12 months. Therefore, the Köppen climate classification for Los Angeles is "*Csa*" representing hot summer and "*Csb*" for Portland meaning cool summer climate. For Portland and Los Angeles, the mean annual temperature is 12.5 °C and 17.7 °C, respectively, and the annual precipitation is 914 mm and 407 mm, respectively.

Chicago has a typical continental climate with hot, humid summers and cold winters, and frequent short fluctuations in temperature, humidity, cloudiness, and wind direction. This type of climate is classified as "*Dfa*". The mean annual temperature of Chicago is 10.8 °C and the annual precipitation is 991 mm.

Denver features a cold semi-arid steppe climate, which is denoted by "*BSk*" in the Köppen climate classification system. It has very low humidity and an average annual precipitation of 360 mm. The mean annual temperature in Denver is 10.4 °C.

Kansas City and Orlando are both in the Köppen climate region of "*Cfa*", which represents a humid, warm temperature subtropical climate. Even if these two cities have the same climate classification, they differ in annual mean temperature and precipitation. Kansas City has a mean annual temperature of 13.7 °C and an annual precipitation of 992 mm. Orlando has a mean annual temperature of 23.0 °C and an annual precipitation of 1,351 mm.

The Köppen climate classification of Phoenix is "*BWh*" which is a hot desert climate that is characterized by long, hot summers, warm transitional seasons, and short, mild to chilly winters. The mean annual temperature is 23.9 °C and the annual precipitation is only 204 mm in Phoenix.

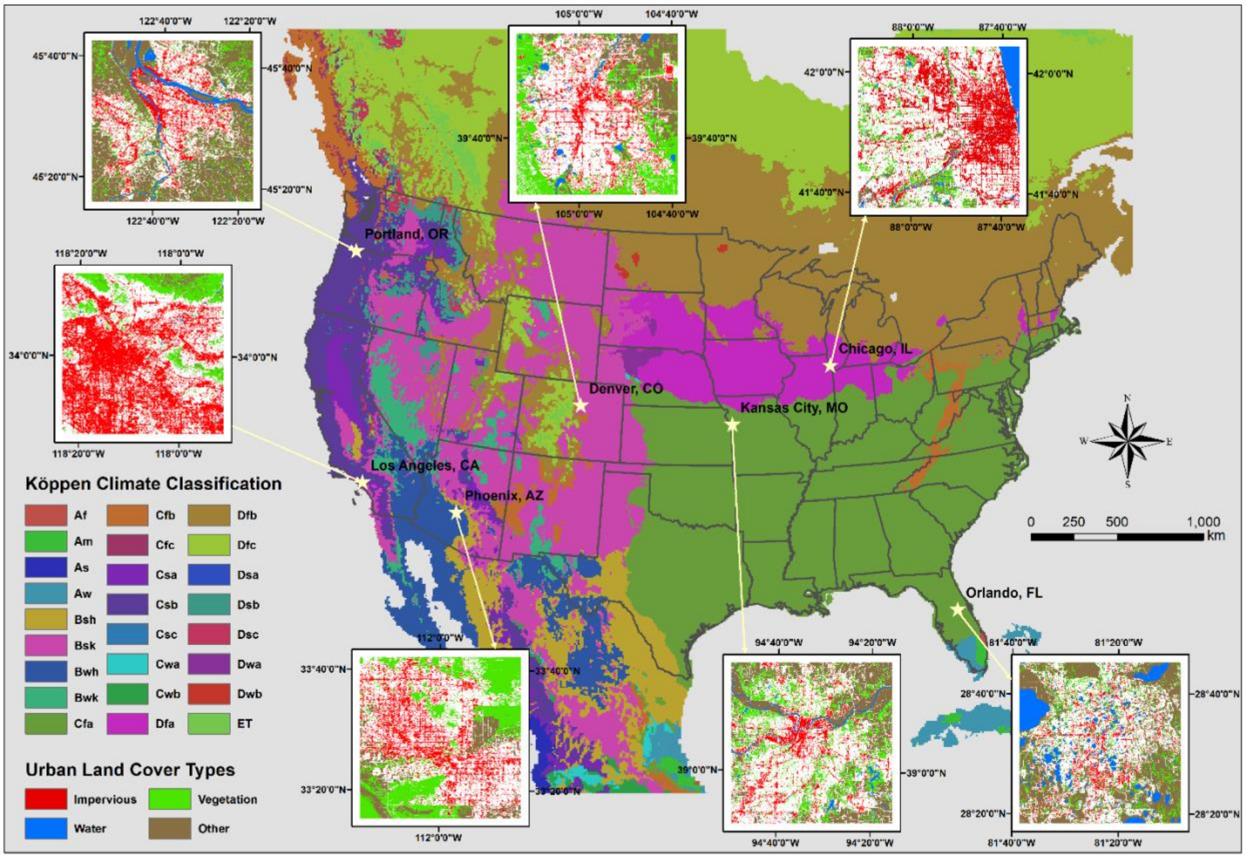

Figure 1. Map showing seven selected metropolitan areas and the Köppen climate classification of the contiguous United States. The legend "Köppen Climate Classification" is for the North America continent and the legend "Urban Land Cover Types" is for seven selected metropolitan inset maps.

Table 1. Population, metropolitan area and climate of seven selected metropolitan areas in the contiguous U.S.

City	State	Population in 2010[a]	Metropolitan area (km^2)[b]	Annual maximum temperature (°C)[c]	Annual minimum temperature (°C)[c]	Annual mean temperature (°C)[c]	Annual precipitation (mm)[c]	Annual mean dew point (°C)[d]	Köppen climate classification
Chicago	Illinois	2,695,598	6,326.7	15.2	6.3	10.8	991	4.4	*Dfa*[1]
Denver	Colorado	600,158	1,730.0	18.3	2.4	10.4	360	-1.1	*BSk*[2]
Kansas City	Missouri	459,787	1,755.6	18.8	8.5	13.7	992	6.7	*Cfa*[3]
Los Angeles	California	3,792,621	4,496.3	22.1	13.2	17.7	407	10.6	*Csa*[4]
Orlando	Florida	238,300	1,548.0	28.0	17.9	23.0	1,351	17.2	*Cfa*[3]
Phoenix	Arizona	1,445,632	2,969.6	30.3	17.4	23.9	204	4.4	*Bwh*[5]
Portland	Oregon	583,776	1,358.2	17.3	7.6	12.5	914	7.2	*Csb*[6]

[1] *Csa*: Mediterranean climate with warm, dry summer
[2] *Dfa*: Continental climate with hot, humid summer
[3] *Bwh*: Hot desert climate
[4] *BSk*: Cold semi-arid climate
[5] *Csb*: Mediterranean climate with cool, dry summer
[6] *Cfa*: Humid subtropical climate with hot summer
Data source: [a] U.S Census Bureau, 2018; [b] U.S. Census Bureau, 2015; [c] U.S. Climate Data, 2019; [d] ClimaTemps, 2017.

3. Data and Methods

3.1 Land cover data

This study derives major urban land cover types from the 2011 National Land Cover Database (NLCD) products that are produced using Landsat imagery by the Multi-Resolution Land Characteristics (MRLC) Consortium, which include land cover classification, percent developed imperviousness, and tree canopy percentage for the entire United States. These products provide nationwide data at 30 m spatial resolution derived from Landsat 5 images. The land cover classification has 20 classes using the USGS Anderson classification system (Anderson, 1976). The overall classification accuracy is 82% at Level II and 88% at Level 1 classes (Wickham et al., 2017). NLCD imperviousness product quantifies urban impervious surface percentage as a continuous variable using the general classification and the regression tree algorithm (Yang et al., 2003). The tree canopy percentage product represents the area that is proportional to tree canopy coverage of each pixel, which is produced using a random forest regression algorithm (Coulston et al., 2012).

3.2 Land surface temperature (LST) data

Moderate Resolution Imaging Spectroradiometer (MODIS) LST 8-day composite product (MOD11A2.V006, version 6) was used during June, July, and August 2011, producing a total of 12 images. MODIS provides an average, 8-day, per pixel LST for both day and night with a spatial resolution of 1,000 m. MODIS LST has been validated within 1 K accuracy using in situ measurements in the range of 263-322 K at an atmospheric column water vapor range of 0.4-3.0 cm (Wan et al., 2002). Only images from 2011 were used to match the NLCD land cover data. Summer months were used because all the cities have relatively warm, dry, clear, and calm weather conditions in the summer, which helps avoid poor data quality due to heavy cloud cover.

3.3 Methods

The method used in this study was to build explanatory models based on the relationship between the clustering of land covers and LST. We chose the explanatory model rather than a predictive model because we wanted to focus exclusively on this one relationship. A predictive model would aim to comprehensively incorporate all factors known to influence LST as independent variables. To build our explanatory model, each of the study area cities were divided into 0.98 km^2 square grids to serve as the basic unit of analysis. This created a set of local-area units where the clustering of land cover could be calculated. To test the relationship of land cover clustering to LST, the Moran's *I* value for each square grid were used for the regression analysis. The following part of this section describes image processing and data analysis (Figure 2).

To simplify the process and to make cities comparable to each other, similar land cover types were grouped together and the focus was mainly on human constructed elements (impervious surface), soil-vegetation continuum (vegetation and open soil), water body, and mixed other types to represent the major elements of an urban landscape, as suggested in the study by Wentz et al. (2018). The reason for grouping vegetation and open soil together is that large areas of pure pixels of barren land and open soil are rarely found in urban developed areas and are more likely to be found in rural areas, such as fallow cropland. Mostly, vegetation cover (e.g. shrub, grass, and scrub) grows on open soils in urban areas; thereby influencing the surface thermal and biophysical properties (Wentz et al., 2018).

The flowchart of image processing and data analysis is shown in Figure 2. A binary image of water body was created by extracting all the water pixels (Class 11) from the NLCD land cover image (MRLC, 2011). A binary impervious surface image was made by selecting all the pixels that have an impervious surface percentage greater than or equal to 60% from the NLCD percent developed imperviousness image, which is considered as a "pure" pixel of imperviousness (Goldblatt et al., 2018). The same rule was also applied to the NLCD tree canopy percentage image, and a binary tree cover image was created using 60% tree cover as the threshold. The tree cover binary image was then combined with NLCD land cover classification Class 52 (shrub/scrub) and Class 71 (grassland/herbaceous) (MRLC, 2011) to create a binary image for vegetation cover. All the other land cover classes in the NLCD classification image were combined together to create a binary image named "mixed".

A summer mean LST image was calculated for both daytime and nighttime by averaging all the 12 MODIS LST images. Summer mean LST images were then resampled to 990 m so that every single LST pixel contained 1,089 land cover pixels (30-m resolution) from the NLCD data. The unit of analysis in this study was therefore a 0.98 km^2 square grid that is converted from MODIS LST pixels. The spatial clustering of land cover was quantified using Moran's *I* within each unit square and then analyzed against the corresponding LST value (Figure 2 and Figure 3). This study is only limited to the use of Moran's *I* rather than landscape metrics and other spatial pattern indicators because the focus was only on spatial clustering of land cover in a small localized urban area. Spatial composition, such as percent area, and pattern analyses, such as fragmentation, were not within the scope of this study.

Moran's *I* is a widely used spatial statistic technique that measures spatial autocorrelation of features based on their locations and attributes (Moran, 1950). Moran's *I* value ranges from -1 to +1, with -1 indicating a perfect dispersion (checkerboard pattern), 0 representing spatial randomness, and +1 meaning a perfect clustering (Table 2). In order to avoid negative values in the subsequent regression analysis and to simplify interpretation, we rescaled original Moran's *I* values to an 8-bit data (on a scale of 0 to 255) using linear interpolation, with values of 0, 127.5, and 255 representing -1, 0, and +1, respectively (Table 2).

As Moran's *I* is calculated for vector data sets, all the binary land cover rasters (water, impervious surface, vegetation, and mixed) were converted to points in the ArcMap software (version 10.6). A Moran's *I* value of each set of land cover points within each 0.98 km^2 square unit of analysis was then calculated. Figure 3 illustrates the relationship between LST and each land cover type and the method to calculate Moran's *I*.

Correlation and multivariate regression analyses were then performed using the summer mean LST as the dependent variable and Moran's *I* values of each land cover as the independent variable. The correlation analysis was done to examine one-to-one relationships, while the multivariate regression was performed to study the combined effects of all the land cover types on LST. The regression equation is formulated as:

$$LST_{d,n} = \beta_0 + \beta_1 I_i + \beta_2 I_v + \beta_3 I_w + \beta_4 I_m + \varepsilon,$$

where $LST_{d,n}$ represents daytime and nighttime summer mean LST; I_i, I_v, I_w and I_m represent Moran's I values of impervious surface, vegetation, water, and mixed type of land cover, respectively; β_0, β_1, β_2, β_3, and β_4 are regression coefficient estimates; and ε is the error term. Only those observations that contained all four land cover types were used in the regression analysis, thereby resulting in less than 2,500 observations for each selected metropolitan area.

Figure 2. Flowchart of image processing and data analysis.

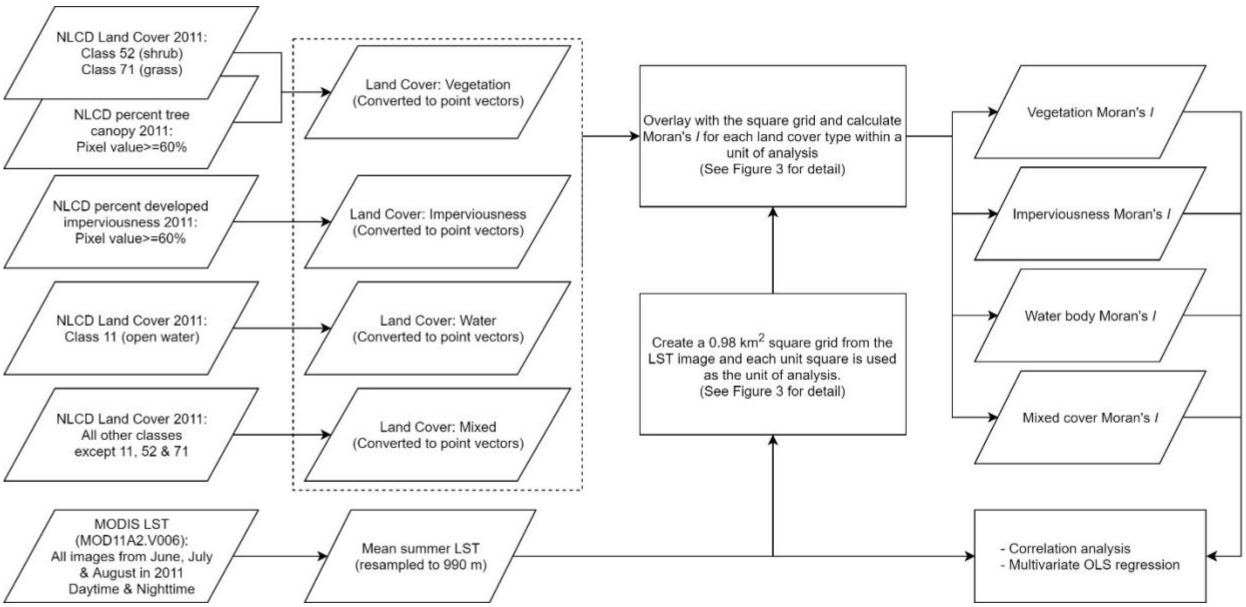

Figure 3. Four hypothetical units of analysis at 0.98 km2 are shown here to illustrate the relationship between the LST value and land cover points and how Moran's *I* values are calculated and rescaled.

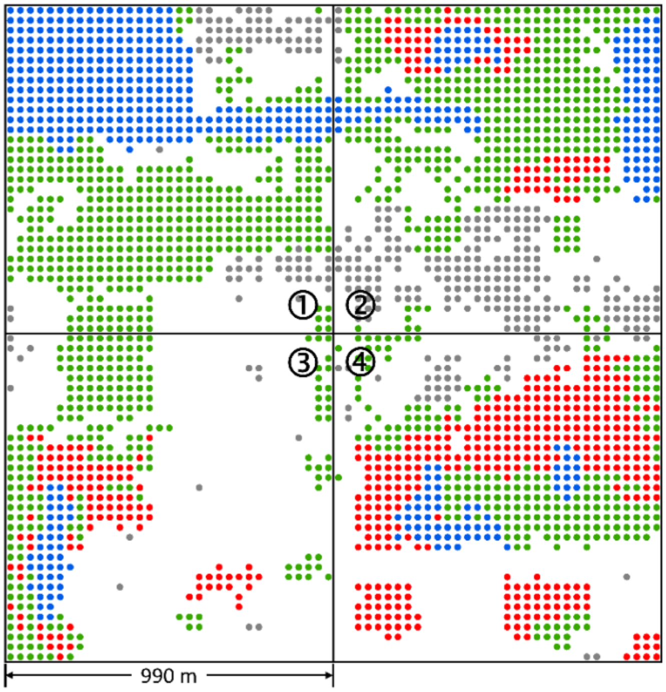

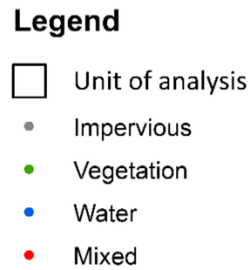

Pixel #	Land Cover	Original Moran's *I*	Rescaled (8-bit) Moran's *I*	*z*-score	*p*-value	Pattern
1	Impervious	0.6206	206.62	28.72	<0.01	Clustered
	Vegetation	0.7349	221.20	33.85	<0.01	Clustered
	Water	0.9087	243.36	41.86	<0.01	Clustered
	Mixed	-	-	-	-	-
2	Impervious	0.6646	212.24	30.66	<0.01	Clustered
	Vegetation	0.6313	207.99	29.08	<0.01	Clustered
	Water	0.7480	222.87	34.53	<0.01	Clustered
	Mixed	0.7358	221.31	33.93	<0.01	Clustered
3	Impervious	0.1373	145.01	6.59	<0.01	Clustered
	Vegetation	0.6182	206.32	28.51	<0.01	Clustered
	Water	0.7556	223.84	35.18	<0.01	Clustered
	Mixed	0.6466	209.94	29.85	<0.01	Clustered
4	Impervious	0.4457	184.32	20.78	<0.01	Clustered
	Vegetation	0.6368	208.69	29.36	<0.01	Clustered
	Water	0.6691	212.81	31.04	<0.01	Clustered
	Mixed	0.7496	223.07	34.53	<0.01	Clustered

Table 2. Illustrations of original and rescaled Moran's *I* values.

Spatial Clustering	Original Moran's *I*	Rescaled (8-bit) Moran's *I*	Graphic example
Perfectly dispersed	-1	0	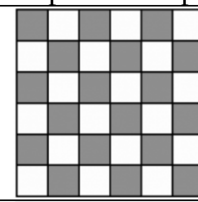
Random	0	127.5	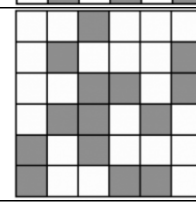
Perfectly clustered	+1	255	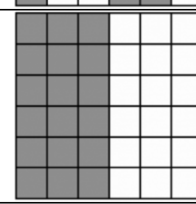

4. Results

4.1 Summary statistics

Table 3 shows the summary statistics of calculated Moran's *I* values and area of each land cover type in each metropolitan area. All the land cover types from all the selected cities have a mean Moran's *I* value greater than 127.5 (e.g., a perfect randomness in Table 2), suggesting highly clustered land covers. However, the spatial composition of land cover types varies significantly across cities. Generally, vegetation cover is the dominant land cover type and its area is larger than impervious surface and water bodies combined, in most cities. The exceptions are Chicago and Los Angeles, which have a larger impervious surface area.

Summary statistics of summer mean LST for each metropolitan area are shown in Table 4. It was found that the range of daytime LST was greater than the range of nighttime LST in all the cities. Phoenix has the highest LST for both daytime and nighttime in the summer because of the hot desert climate, while Portland has the lowest LST among all the cities due to its cool summer Mediterranean climate.

4.2 Relationship between spatial clustering of land cover types and LST

The correlation coefficients between the spatial clustering of land cover types and LST are shown in Table 5. Moran's *I* of impervious surface has a highly significant positive relationship with LST for both daytime and nighttime, indicating a strong warming effect of clustered impervious surfaces. Moran's *I* of vegetation cover is negatively correlated with LST for both daytime and nighttime, which indicates that the spatially clustered vegetation cover has a cooling effect. Moreover, in most cities, clustered water bodies have a cooling effect during the day, but a warming effect at night, except for Phoenix. Mixed types of land cover generally show a negative correlation with LST in most cities but not many results are statistically significant.

Table 6 shows multivariate regression analysis results, and Figure 4 is the visualization of coefficient estimates that are statistically significant at the 0.05 level only. This is the combined effect of spatial clustering of all the land cover types on LST, which is different from the relationships examined in the correlation analysis. The coefficient of determination (R^2) indicates the percentage of variation in LST that can be explained by the regression model built using urban land cover Moran's *I* values. The R^2 values are <0.3, and all the models are statistically significant at the 0.05 level except the nighttime model for Los Angeles, which is only significant at the 0.1 level. The variance inflation factor (VIF) of all the variables is between 1 and 2, which means that the models are unlikely to have a multicollinearity issue. The models, which focus exclusively on the relationship between land cover clustering and LST exclude predictive variables, such as the areas of land covers. This means that the R^2, which might be considered low for predictive models, shows a percentage of the variation that is explained by spatial clustering. Thus, 15% to 33% of the variation in LST can be explained simply by the clustering effects of land covers (Table 6).

Coefficient estimates of the Moran's *I* values of impervious surfaces are statistically significantly and positive except for Phoenix. This suggests that clustered impervious surfaces could elevate LST for both daytime and nighttime in most cities, regardless of the regional background climate of a city. This result is consistent with the correlation analysis shown in Table 5. Moreover, the daytime coefficient estimate is greater than the nighttime coefficient for most cities, indicating that the warming effect of clustered impervious surface is stronger during the daytime than the nighttime. Los Angeles (β_1=0.036, p<0.01) and Portland (β_1=0.030, p<0.01)have the largest coefficient estimates of impervious surface Moran's I for the daytime among all the cities, while Kansas City (β_1=0.013, p<0.01) and Chicago (β_1=0.012, p<0.01) have the largest coefficient estimates for the nighttime (Table 6 & Figure 4).

Negative relationships are found between Moran's I values of vegetation cover and LST in some cities, but the magnitude varies. Only Phoenix and Portland have a statistically significant and negative relationship between the cluster of vegetation cover and LST for both daytime and nighttime, which means the more clustered the vegetation cover is, the lower the LST would be. Moreover, the cooling effect of clustered vegetation cover is stronger in the daytime than the nighttime. The strongest cooling effect of vegetation is found in Kansas City for the daytime (β_2=-0.030, p<0.01) and in Denver for the nighttime (β_2=-0.014, p<0.01). The cooling effect of vegetation cover in urban environments are only found in dry and temperate climate regions, but not in continental climate regions.

Similar to the correlation analysis results in Table 5, Moran's I of water body consistently shows a significant negative relationship with LST during the day, but a positive relationship during the night in most cities except for Los Angeles and Phoenix, and this effect is found in temperate, dry, and continental climate regions. This is because Los Angeles and Phoenix are both naturally scarce in water resources and large water bodies. Moreover, the cooling effect of clustered water bodies during the day is stronger than the warming effect at night, as the absolute value of the coefficient estimates for the daytime is greater than that for the nighttime. Portland has the largest coefficient value during the day (β_3=-0.043, p<0.01), while Denver has the largest value during the night (β_3=0.008, p<0.01).

A statistically significant relationship between the spatial clustering of mixed land cover types and LST is rare but when it is significant, the relationship is negative, that is, the mixed land cover types generally have a cooling effect on LST for both daytime and nighttime. The effect, however, is weaker than that of vegetation and water during the daytime and weaker than vegetation at night. Its detailed mechanism is difficult to explain due to the uncertain spatial composition of different land cover types.

Table 3. Summary statistics of Moran's *I* values (8-bit on a scale of 0 to 255, unitless) and the area of each land cover type of each metropolitan area.

City	Köppen climate	Land cover type	Max.	Min.	Mean	Range	Std. Dev.	Area (km^2)
Chicago	*Dfa*	Impervious	244.97	127.13	203.56	117.84	21.18	697.55
		Vegetation	249.46	126.75	214.80	122.71	30.24	227.44
		Water	249.42	126.81	204.13	122.61	24.68	113.90
		Mixed	245.71	127.25	204.39	118.46	22.99	120.30
Denver	*BSk*	Impervious	242.08	126.68	184.63	115.40	22.97	336.90
		Vegetation	249.82	126.62	200.73	123.19	26.69	558.41
		Water	247.89	127.31	207.17	120.58	27.76	51.48
		Mixed	249.25	127.06	200.91	122.19	22.32	398.79
Kansas City	*Cfa*	Impervious	249.38	125.99	189.23	123.40	26.78	263.40
		Vegetation	243.45	126.62	196.92	116.83	26.50	402.25
		Water	248.96	127.31	205.69	121.65	26.39	55.62
		Mixed	248.40	127.31	216.59	121.09	16.99	621.83
Los Angeles	*Csa*	Impervious	242.21	126.56	196.89	115.66	19.70	1,092.56
		Vegetation	240.49	127.00	184.62	113.49	21.59	289.48
		Water	241.79	126.75	188.08	115.04	28.47	5.36
		Mixed	242.76	127.37	184.44	115.39	18.71	62.00
Orlando	*Cfa*	Impervious	242.25	126.68	189.96	115.56	28.17	169.81
		Vegetation	248.51	127.13	209.17	121.38	17.54	689.43
		Water	249.84	127.31	213.27	122.53	26.66	251.49
		Mixed	249.48	127.19	209.64	122.29	17.85	855.11
Phoenix	*BWh*	Impervious	243.13	126.37	187.53	116.76	20.85	462.57
		Vegetation	247.04	127.31	197.14	119.73	22.83	611.49
		Water	243.36	127.31	194.64	116.05	23.54	10.32
		Mixed	248.83	127.25	204.86	121.58	23.71	250.17
Portland	*Csb*	Impervious	247.63	126.62	192.31	121.01	27.99	311.29
		Vegetation	247.03	126.56	203.57	120.48	24.01	662.97
		Water	249.45	127.31	211.82	122.13	30.28	97.33
		Mixed	246.08	127.19	206.70	118.90	18.23	1,044.70

Table 4. Summary statistics of summer mean LST for each metropolitan area.

City	Köppen climate	LST	Max. (°C)	Min. (°C)	Mean (°C)	Range (°C)	Std. Dev.
Chicago	*Dfa*	daytime	37.04	19.09	32.68	17.96	2.65
		nighttime	23.58	18.12	21.29	5.46	0.87
Denver	*BSk*	daytime	42.81	26.48	38.63	16.33	2.38
		nighttime	20.68	13.10	17.34	7.59	1.47
Kansas City	*Cfa*	daytime	38.28	27.72	32.58	10.56	2.15
		nighttime	25.09	20.31	22.95	4.78	1.06
Los Angeles	*Csa*	daytime	44.24	26.93	38.76	17.31	3.39
		nighttime	19.73	14.87	17.69	4.85	0.82
Orlando	*Cfa*	daytime	39.31	26.39	33.30	12.91	2.60
		nighttime	26.61	20.84	23.37	5.77	0.98
Phoenix	*Bwh*	daytime	54.06	43.36	48.84	10.70	1.51
		nighttime	32.29	25.09	29.03	7.21	1.17
Portland	*Csb*	daytime	36.05	18.28	27.91	17.77	3.57
		nighttime	17.33	10.37	13.11	6.96	1.04

Table 5. Correlation coefficients between Moran's *I* values of different land cover types and LST.

City	Köppen climate	Land cover type	Correlation coefficient (daytime LST)	Correlation coefficient (nighttime LST)
Chicago	*Dfa*	Impervious	0.191**	0.266**
		Vegetation	-0.354**	-0.292**
		Water	-0.230**	0.193**
		Mixed	-0.005	-0.041
Denver	*BSk*	Impervious	0.179**	0.306**
		Vegetation	-0.121**	-0.223**
		Water	-0.346**	-0.046
		Mixed	0.164**	-0.068**
Kansas City	*Cfa*	Impervious	0.400**	0.449**
		Vegetation	-0.540**	-0.425**
		Water	-0.047	0.165**
		Mixed	-0.045	-0.120**
Los Angeles	*Csa*	Impervious	0.204**	0.182**
		Vegetation	-0.033	-0.161**
		Water	-0.012	0.200*
		Mixed	-0.248**	-0.006
Orlando	*Cfa*	Impervious	0.270**	0.232**
		Vegetation	-0.070**	-0.098**
		Water	-0.168**	0.198**
		Mixed	-0.139**	-0.081**
Phoenix	*BWh*	Impervious	0.179**	0.073**
		Vegetation	-0.136**	-0.054*
		Water	0.030	0.012
		Mixed	-0.084**	-0.141**
Portland	*Csb*	Impervious	0.328**	0.423**
		Vegetation	-0.208**	-0.248**
		Water	-0.317**	0.2068**
		Mixed	0.030	0.0230

** Correlation coefficients that are statistically significant at the 0.01 level.
* Correlation coefficients that are statistically significant at the 0.05 level.

Table 6. Multivariate regression analysis results.

City	Köppen climate	LST	Impervious Moran's *I*, β_1	Vegetation Moran's *I*, β_2	Water Moran's *I*, β_3	Mixed Moran's *I*, β_4	R^2	Model *p*-value	VIF			
									Impervious	Vegetation	Water	Mixed
Chicago	*Dfa*	daytime	0.027**	-0.007	-0.018**	-0.004	0.164	<0.01	1.01	1.06	1.01	1.06
		nighttime	0.012**	0.000	0.006**	-0.001	0.167	<0.01				
Denver	*BSk*	daytime	0.011*	-0.006	-0.021**	0.003	0.133	<0.01	1.01	1.00	1.01	1.01
		nighttime	0.011**	-0.014**	0.008**	0.001	0.203	<0.01				
Kansas City	*Cfa*	daytime	0.022**	-0.030**	-0.004	-0.013**	0.304	<0.01	1.04	1.05	1.01	1.01
		nighttime	0.013**	-0.003	0.005**	-0.011**	0.303	<0.01				
Los Angeles	*Csa*	daytime	0.036**	-0.028	-0.018	0.003	0.330	<0.01	1.07	1.07	1.02	1.00
		nighttime	0.009*	-0.006	0.000	0.007	0.163	<0.1				
Orlando	*Cfa*	daytime	0.018**	0.001	-0.009**	-0.025**	0.136	<0.01	1.00	1.81	1.04	1.81
		nighttime	0.005**	-0.002	0.004**	-0.008**	0.157	<0.01				
Phoenix	*BWh*	daytime	0.000	-0.016**	0.006	-0.002	0.058	<0.05	1.01	1.02	1.89	1.93
		nighttime	0.004	-0.008*	0.010	-0.017**	0.148	<0.01				
Portland	*Csb*	daytime	0.030**	-0.027**	-0.043**	0.015	0.236	<0.01	1.03	1.25	1.00	1.22
		nighttime	0.009**	-0.011**	0.004**	-0.000	0.188	<0.01				

** Coefficient estimates that are statistically significant at the 0.01 level.

* Coefficient estimates that are statistically significant at the 0.05 level.

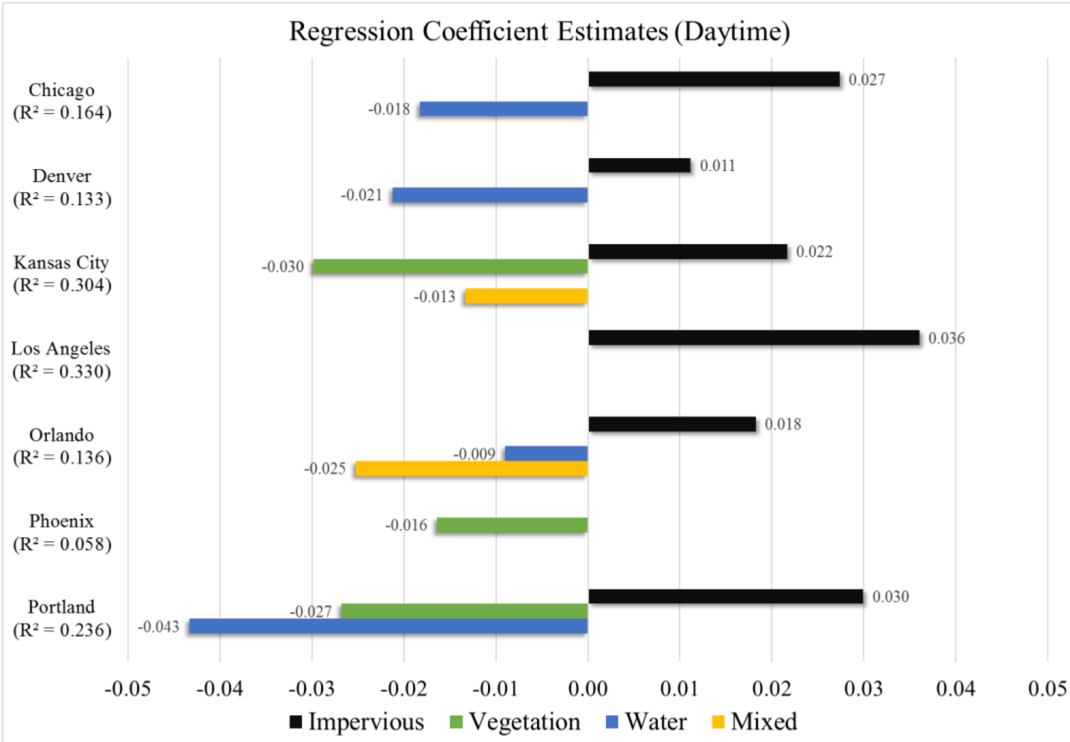

(a)

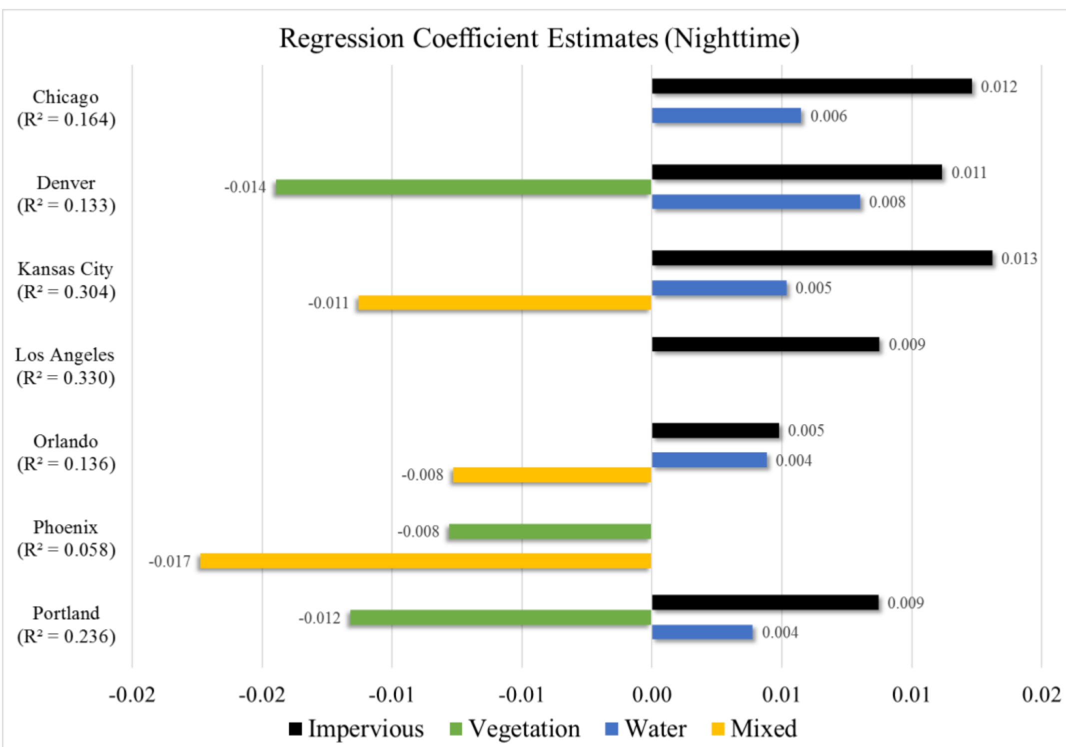

(b)

Figure 4. The visualization of regression coefficient estimates for each metropolitan area.

5. Discussion

The intent of this study was to quantify the effects of urban land cover clusters on LST in small localized area across cities in the contiguous U.S. with different background climate conditions. Multivariate regression analysis results in Table 6 show that all the models are statistically significant, which indicates that these models can be used to explain the empirical relationship between spatial clustering of land covers and LST. Given the specific focus to understand the role that spatial clustering plays on LST, variables known to potentially influence LST, such as spatial composition (e.g. land cover area or percent area) and spatial configuration variables (e.g. abundance, shape, connectivity, etc.) were excluded. Including these variables would likely result in higher R^2 values but diminish the ability to examine the effect of spatial clustering. In the following sections, the effect of spatial clustering of each land cover on LST have been examined and policy recommendations have been put forward based on the results.

5.1 Spatial clustering of impervious surfaces and LST

Spatial clustering of impervious surfaces plays an important role in controlling LST for both day and night in small localized urban areas. It was found that clustered impervious surfaces elevate LST, indicating a warming effect in most climate regions. This warming effect is stronger during the daytime than the nighttime in all the temperate and continental climate regions, especially in Mediterranean climate regions such as *Csa* (Los Angeles) and *Csb* (Portland) (Table 6). This is because clustered impervious surfaces increase ground heat fluxes and sensible heat fluxes during the daytime by efficiently converting shortwave radiation from the solar energy into longwave radiation to heat up the lower atmosphere quickly, but reduce latent heat fluxes by decreasing evapotranspiration from soil-vegetation systems (Oke, 1982; Ma et al., 2016). Furthermore, clustered impervious surfaces can also indirectly augment anthropogenic heat emissions from transportation, industries, and building infrastructure, all of which lead to increased LST (Zhang et al., 2010; Zhou et al., 2014; Kuang et al., 2015). During the night, anthropogenic heat becomes impervious surfaces' main energy source due to the loss of solar energy, which significantly decreases the efficiency of energy transfer. Therefore, LST drops significantly after sunset.

This phenomenon is not found in the dry desert climate region of Phoenix. This result contradicts Myint et al. (2015), who studied spatial patterns of paved surfaces and buildings in desert cities and found significant positive relationships of impervious clusters with elevated LST. It is anticipated that this difference is related to the convection efficiency in dry climates. Zhao et al. (2014) found that rough urban land can enhance convection efficiency and lower aerodynamic resistance in dry climate zones, resulting in a cooling effect, while convection is less efficient at dissipating heat from urban land in the humid climate, leading to a warming effect. Although our findings do not suggest a cooling effect of clustered impervious surface in dry climate regions, such as *BSk* and *BWh*, the warming effect is much weaker than other climate regions and this effect is not even statistically significant in the hot desert climate (*BWh*).

5.2 Spatial clustering of vegetation cover and LST

It is widely accepted that clustered vegetation cover effectively lowers LST in urban environments (Yokohari et al., 1997; Zhang et al., 2009; Li et al., 2012). In this study, however, clustered vegetation cover only showed significant cooling effect for Phoenix and Portland for both daytime and nighttime; this was not significant in other cities in other Köppen climate regions. Therefore, understanding the impact of spatial clustering of greenspaces on LST in urban environments is a more complicated mechanism (Bowler et al., 2010; Armson, 2012; Zhang et al. 2017; Zhao et al. 2018).

The findings in this study agree with other studies, indicating that the influence of vegetation clusters on LST does exist in the desert climate. Zhang et al. (2017) demonstrated that in the hot desert climate, clustered greenspaces enhance the cooling effect at a local scale, such as in small urban parks, but dispersed greenspaces show a better local cooling effect, overall. Zhao et al. (2018) showed that both clustered and evenly arranged trees provide significant cooling benefits to the entire residential area. Myint et al. (2015) also found a negative relationship between Moran's *I* values and LST in Phoenix for grass and trees. Fan et al. (2015) used different percentages of tree cover and grass cover in Phoenix and found negative relationship between Moran's *I* and LST for all the percentage categories.

The results also showed that clustered vegetation cover does not effectively lower LST during the day or night in Chicago, Los Angeles, and Orlando. Zhou et al. (2011) claimed that a clustered woody vegetation would even elevate LST when quantifying the spatial pattern using mean nearest neighbor distance (MNND) method. Although, a positive relationship between clustered vegetation and LST was not established in this study, the actual effect of the spatial clustering of greenspaces on LST really depends on the background climate. In climate regions with hot, humid summer, such as Chicago and Orlando, higher atmospheric moisture and highly clustered vegetation cover could slow down the overall evapotranspiration rate and offset the cooling benefits from vegetation. Similar results are also reported for Hong Kong (Tan et al., 2016) and Singapore (Hwang et al., 2015).

5.3 Spatial clustering of water bodies and LST

The effects of spatial clustering of water bodies on LST is reversed because of the higher specific heat capacity of water compared to other materials in urban environments, such as anthropogenic materials and open soils. These materials' surface temperature far exceeds water bodies during the daytime by quickly absorbing shortwave radiation from solar energy. Moreover, they emit heat through longwave radiation after sunset and their temperature drops quickly. Water bodies' temperature remains relatively constant during the entire day. Therefore, the spatial clustering of water bodies shows a cooling effect during the daytime, but a potential warming effect at night, especially during the winter (Oke, 1982; Kim, 1992; Wang et al., 2018). Furthermore, the warming effect of clustered water bodies during the night is much weaker than that of impervious surface in all the cities (Figure 4b). Even though clustered water elevates LST during the night, it has a more positive impact in reducing daytime LST in urban environments.

There is no evidence from this study to show that clustered water bodies can influence LST in the daytime or nighttime in drier climates, such as Los Angeles or Phoenix. In Los Angeles, water bodies are naturally scare, and the atmospheric humidity reaches the lowest during summers. This is due to its Mediterranean climate with dry, warm summers. Despite its desert location, Phoenix has more water bodies across the metro area (Table 3), mostly in the form of small artificial lakes in golf courses, parks, private gardens and residential communities. Even though these small water bodies are spatially clustered, they are not sufficient to have a significant influence on local climate and to cool down surface temperature because of the subtropical desert climate with extremely hot summer, low annual rainfall, low relative humidity, and low dew point.

5.4 Policy recommendations

Recently there have been substantial resources devoted to exploring and implementing mitigation strategies for urban heat. Many studies suggest that building larger greenspaces but smaller size of impervious surface when planning new developed areas can potentially reduce urban warming and mitigate the UHI effect (Buyantuyev and Wu, 2010; Zhou et al., 2011; Li et al., 2012; Kong et al., 2014; Taleghani et al., 2014; Zheng et al., 2014; Fan et al., 2015; Myint et al., 2015; Wang et al., 2016; Yang et al., 2016; Estoque et al., 2017; Gage and Cooper, 2017; Nor et al., 2017; Yang and Wang, 2017). This study built on these policy guidelines by suggesting means to spatially organize greenspaces, impervious surfaces, and water bodies in the face of urban population growth. This requires housing, workspace, transportation, and infrastructure development. Additionally, the authors added to these recommendations by quantifying how the regional climate background of different cities should be considered when assessing the spatial clustering of urban land covers. Whereas, a smaller impervious surface area, which is deemed as ideal by other studies, is often impractical. This study found that more dispersed impervious surface patches can potentially alleviate excessive urban warming in most cities of the U.S. This is also evident across different climate regions, but is less effective for hot desert cities such as Phoenix and Las Vegas. Similarly, building more clustered greenspaces can potentially reduce LST in warm, dry, and temperate regions, but may not work well in some regions with continental (e.g. Chicago), cold semi-arid (e.g. Denver), and humid subtropical climates (e.g. Orlando).

Urban sprawl has been described as a “territorial disease” because of the rampant growth effect (EEA, 2006; Worldwatch Institute, 2013; Barrington-Leigh and Millard-Ball, 2015; Paleari, 2017; Romano et al., 2017). Even though building smaller area and more dispersed impervious surfaces can potentially reduce urban heating and alleviate the UHI effect, it is still unsustainable as it may threaten both the natural and rural environments, raising more greenhouse gas emissions, creating more air and noise pollutions, and causing less efficient energy use (EEA, 2006). Thus, this study suggests that cities should adopt sustainable practices, such as green roofs when planning for new development areas. Green roofs can not only provide cooling in build environment, but also have great potentials in protecting water resources and conserving energy (Deardorff, 1978; Del Barrio, 1998; Theodosiou, 2003; DeNardo et al., 2005; Kumar and Kaushik, 2005; Sailor, 2008).

Building cities around spatially clustered water bodies can be a double-edged sword due to its significant warming effect at night, but it could be a good practice for reducing urban warming during the daytime. Therefore, this study suggests that urban areas should include greenspaces around dispersed water bodies and clustered greenspaces so that the vegetation’s cooling effect at night would somewhat offset the warming of water bodies nearby. However, this strategy may not work well for cities with warm and dry summers, such as Los Angeles and Phoenix. It is more challenging to adapt the above policy recommendations to existing developed areas, but it can be effectively applied when planning for new urbanized areas.

6. Conclusions

Previous studies have quantified the relationship between spatial composition and configuration of land covers and LST for many cities around the world; however, the impact of spatial clustering of land covers on LST remains less understood. The concept of spatial clustering is essential to urban planning and design because it measures the spatial distribution and organization of urban land covers, which has been suggested to have a potential influence on urban climate. In addition, the regional climate background of a city also plays an important role in influencing the relationship between the spatial clustering of land covers and LST, which is another factor that is often neglected by numerous studies. Thus, this study makes a new contribution to the literature and knowledge by exploring the empirical relationship between spatial clustering of urban land cover types and LST in seven large metropolitan areas in the contiguous United States having different climate backgrounds. The goal was to build results and to develop strategies that are generalizable across a larger geographic region than what can be derived from one case study of a city within a limited area.

Results show that the actual impact of spatial clustering of urban land covers on LST varies significantly across different Köppen climate regions in the U.S. Based on research findings, this study suggested that the spatial arrangement of impervious surfaces, greenspaces, and water bodies is another important factor that controls urban heating and cooling, which can be considered as a new mitigation strategy to the UHI effect. Policy recommendations have also been provided to urban planners, developers, and managers with respect to optimizing the spatial organization of different land covers when planning for new developed areas. However, the implementation of such a policy has to take the regional climate background into consideration as well. These suggestions may not only be useful to the cities in the U.S., but may also have the potential to be applicable to other cities around the world having similar climate background.

Future studies are needed to explore the engineering and physical mechanisms behind these findings to understand why and how spatial clustering of urban land covers influence LST at a local scale. This requires a significant amount of interdisciplinary efforts from climatologists, meteorologists, environmentalists, physicists, engineers, and geographers. In addition, more research should be done to understand how urban morphology, such as building height and shape, influences urban warming. Furthermore, with the availability of remotely sensed data that cover the entire world, on the methodology of this study can be applied to a global scale to provide a further understanding of how spatial clustering of urban land cover influences urban warming in cities with different climate backgrounds.

References

Akbari, H., Pomerantz, M., & Taha, H. (2001). Cool surfaces and shade trees to reduce energy use and improve air quality in urban areas. *Solar Energy, 70(3),* 295-310.

Anderson, J. R. (1976). *A land use and land cover classification system for use with remote sensor data*. US Government Printing Office, *964*.

Armson, D. (2012). *The effect of trees and grass on the thermal and hydrological performance of an urban area*. Ph.D. dissertation. University of Manchester.

Ashie, Y., Ca, V. T., & Asaeda, T. (1999). Building canopy model for the analysis of urban climate. *Journal of Wind Engineering and Industrial Aerodynamics, 81*(1-3), 237-248.

Barrington-Leigh, C., & Millard-Ball, A. (2015). A century of sprawl in the United States. *Proceedings of the National Academy of Sciences*, *112*(27), 8244-8249.
Bowler, D. E., Buyung-Ali, L., Knight, T. M., & Pullin, A. S. (2010). Urban greening to cool towns and cities: A systematic review of the empirical evidence. *Landscape and Urban Planning*, *97*(3), 147-155.
Brown, R. D., Vanos, J., Kenny, N., & Lenzholzer, S. (2015). Designing urban parks that ameliorate the effects of climate change. *Landscape and Urban Planning*, *138*, 118-131.
Buyantuyev, A., & Wu, J. (2010). Urban heat islands and landscape heterogeneity: linking spatiotemporal variations in surface temperatures to land-cover and socioeconomic patterns. *Landscape Ecology*, *25*(1), 17-33.
Ca, V.T., Asaeda, T., & Abu, E.M. (1998). Reductions in air conditioning energy caused by a nearby park. *Energy and Buildings*, *29*(1), 83-92.
Carlson, T.N., & Arthur S.T. (2000). The impact of land use - land cover changes due to urbanization on surface microclimate and hydrology: A satellite perspective. *Global and Planetary Change*, *25*(1-2), 49-65.
Chen, Y., Chiu, H., Su, Y., Wu, Y., & Cheng, K. (2017). Does urbanization increase diurnal land surface temperature variation? Evidence and implications. *Landscape and Urban Planning*, *157*, 247-258.
Cleland, E. E., Chuine, I., Menzel, A., Mooney, H. A., & Schwartz, M. D. (2007). Shifting plant phenology in response to global change. *Trends in Ecology & Evolution*, *22*(7), 357-365.
ClimaTemps. (2017). *Climate, Average Weather of USA*. Retrieved January 7, 2019 from http://www.usa.climatemps.com/
Coulston, J. W., Moisen, G. G., Wilson, B. T., Finco, M. V., Cohen, W. B., & Brewer, C. K. (2012). Modeling percent tree canopy cover: a pilot study. *Photogrammetric Engineering & Remote Sensing*, *78*(7), 715-727.
Cuzick, J., & Edwards, R. (1990). Spatial clustering for inhomogeneous populations. *Journal of the Royal Statistical Society: Series B (Methodological)*, *52*(1), 73-104.
Deardorff, J. W. (1978). Efficient prediction of ground surface temperature and moisture, with inclusion of a layer of vegetation. *Journal of Geophysical Research: Oceans*, *83*(C4), 1889-1903.
Del Barrio, E. P. (1998). Analysis of the green roofs cooling potential in buildings. *Energy and Buildings*, *27*(2), 179-193.
DeNardo, J. C., Jarrett, A. R., Manbeck, H. B., Beattie, D. J., & Berghage, R. D. (2005). Stormwater mitigation and surface temperature reduction by green roofs. *Transactions of the ASAE*, *48*(4), 1491-1496.
Essa. W., Kwast, J., Verbeiren, B., & Batelaan, O. (2013). Downscaling of thermal images over urban areas using the land surface temperature-impervious percentage relationship. *International Journal of Applied Earth Observation and Geoinformation*, *23*, 95-108.
Estoque, R. C., Murayama, Y., & Myint, S. W. (2017). Effects of landscape composition and pattern on land surface temperature: An urban heat island study in the megacities of Southeast Asia. *Science of the Total Environment*, *577*, 349-359.
European Environment Agency (2006). *Urban sprawl in Europe: The ignored challenge. Report No. 10/2006*. Copenhagen, Denmark: European Environment Agency.
Fan, C., & Myint, S. W. (2014). A comparison of spatial autocorrelation indices and landscape metrics in measuring urban landscape fragmentation. *Landscape and Urban Planning*, *121*, 117-128.

Fan, C., Myint, S. W., & Zheng, B. (2015). Measuring the spatial arrangement of urban vegetation and its impacts on seasonal surface temperatures. *Progress in Physical Geography, 39*(2), 199-219.

Gage, E. A., & Cooper, D. J. (2017). Relationships between landscape pattern metrics, vertical structure and surface urban Heat Island formation in a Colorado suburb. *Urban Ecosystems, 20*(6), 1229-1238.

Goldblatt, R., Stuhlmacher, M. F., Tellman, B., Clinton, N., Hanson, G., Georgescu, M., Wang, C., Serrano-Candela, F., Khandelwal, A. K., Cheng, W.-H., & Balling, R. C. (2018). Using Landsat and nighttime lights for supervised pixel-based image classification of urban land cover. *Remote Sensing of Environment, 205*, 253-275.

Guhathakurta, S., & Gober, P. (2007). The impact of the Phoenix urban heat island on residential water use. *Journal of the American Planning Association, 73*(3), 317-329.

Gustafson, E. J. (1998). Quantifying landscape spatial pattern: what is the state of the art? *Ecosystems*, *1*(2), 143-156.

Hwang, Y. H., Lum, Q. J. G., & Chan, Y. K. D. (2015). Micro-scale thermal performance of tropical urban parks in Singapore. *Building and Environment, 94*, 467-476.

Kalkstein, L. S., & Smoyer, K. E. (1993). The impact of climate change on human health: some international implications. *Experientia, 49*(11), 969-979.

Kalnay, E., & Cai, M. (2003). Impact of urbanization and land-use change on climate. *Nature, 423*(6939), 528.

Karnieli, A., Agam, N., Pinker, R. T., Anderson, M., Imhoff, M. L., Gutman, G. G., Panov, N., & Goldberg, A. (2010). Use of NDVI and land surface temperature for drought assessment: Merits and limitations. *Journal of Climate*, *23*(3), 618-633.

Kim, H. H. (1992). Urban heat island. *International Journal of Remote Sensing*, *13*(12), 2319-2336.

Kinney, P., Shindell, D., Chae, E., & Winston, B. (2001). *Climate change and public health: Impact assessment for the NYC metropolitan region*. In: Rosenzweig, C., Solecki W.D. (eds) Climate Change and a Global City: An Assessment of the Metropolitan East Coast Region. Columbia Earth Institute, New York.

Kolokotroni, M., Ren, X., Davies, M., & Mavrogianni, A. (2012). London's urban heat island: Impact on current and future energy consumption in office buildings. *Energy and Buildings*, *47*, 302-311.

Kong, F., Yin, H., James, P., Hutyra, L. R., & He, H. S. (2014). Effects of spatial pattern of greenspace on urban cooling in a large metropolitan area of eastern China. *Landscape and Urban Planning*, *128*, 35-47.

Kottek, M., Grieser, J., Beck, C., Rudolf, B., & Rubel, F. (2006). World map of the Köppen-Geiger climate classification updated. *Meteorologische Zeitschrift, 15*(3), 259-263.

Kuang, W., Liu, Y., Dou, Y., Chi, W., Chen, G., Gao, C., Yang, T., Liu, J., & Zhang, R. (2015) What are hot and what are not in an urban landscape: quantifying and explaining the land surface temperature pattern in Beijing, China. *Landscape Ecology, 30*(2), 357–373.

Kumar, R., & Kaushik, S. C. (2005). Performance evaluation of green roof and shading for thermal protection of buildings. *Building and Environment*, *40*(11), 1505-1511.

Lambin, E. F., Turner B.L., Geist, H.J., Agbola, S.B., Angelsen, A., Bruce, J.W., & Xu, J. (2001). The causes of land-use and landcover change: moving beyond the myths. *Global Environmental Change, 11*, 261-269.

Li, X., Zhou, W., Ouyang, Z., Xu, W., & Zheng, H. (2012). Spatial pattern of greenspace affects land surface temperature: evidence from the heavily urbanized Beijing metropolitan area, China. *Landscape Ecology, 27*(6), 887-898.

Ma, Q., Wu, J., & He, C. (2016). A hierarchical analysis of the relationship between urban impervious surfaces and land surface temperatures: spatial scale dependence, temporal variations, and bioclimatic modulation. *Landscape Ecology, 31*, 1139-1153.

Macintyre, H. L., Heaviside, C., Taylor, J., Picetti, R., Symonds, P., Cai, X. M., & Vardoulakis, S. (2018). Assessing urban population vulnerability and environmental risks across an urban area during heatwaves – Implications for health protection. *Science of the Total Environment, 610*, 678-690.

Masoudi, M., Tan, P. Y., & Liew, S. C. (2019). Multi-city comparison of the relationships between spatial pattern and cooling effect of urban green spaces in four major Asian cities. *Ecological Indicators*, *98*, 200-213.Miao, Z., Chen, Y., Zeng, X., & Li, J. (2016). Integrating spatial and attribute characteristics of extended Voronoi diagrams in spatial patterning research: A case study of Wuhan city in China. *International Journal of Geo-Information, 5*(7), 120.

Morabito, M., Crisci, A., Messeri, A., Orlandini, S., Raschi, A., Maracchi, G., & Munafò, M. (2016). The impact of built-up surfaces on land surface temperatures in Italian urban areas. *Science of the Total Environment*, *551*, 317-326.

Moran, P. A. (1950). Notes on continuous stochastic phenomena. *Biometrika*, *37*(1/2), 17-23.

Multi-Resolution Land Characteristics Consortium (MRLC). (2011). National Land Cover Database 2011 (NLCD2011) Legend. Retrieved January 7, 2019 from: https://www.mrlc.gov/data/legends/national-land-cover-database-2011-nlcd2011-legend

Myint, S. W., Zheng, B., Talen, E., Fan, C., Kaplan, S., Middel, A., Smith, M., Huang, H.-P., & Brazel, A. (2015). Does the spatial arrangement of urban landscape matter? Examples of urban warming and cooling in Phoenix and Las Vegas. *Ecosystem Health and Sustainability*, *1*(4), 1-15.

Nie, Q., & Xu, J. (2015). Understanding the effects of the impervious surfaces pattern on land surface temperature in an urban area. *Frontiers of Earth Science*, *9*(2), 276-285.

Nor, A. N. M., Corstanje, R., Harris, J. A., & Brewer, T. (2017). Impact of rapid urban expansion on green space structure. *Ecological Indicators*, *81*, 274-284

Oke, T. R. (1982). The energetic basis of the urban heat island. *Quarterly Journal of the Royal Meteorological Society, 108*(455), 1-24.

Oke. T. R. (1987). *Boundary Layer Climates*. New York, New York: Routledge.

Paleari, S. (2017). Is the European Union protecting soil? A critical analysis of Community environmental policy and law. *Land Use Policy*, *64*, 163-173.Romano, B., Zullo, F., Fiorini, L., Marucci, A., & Ciabò, S. (2017). Land transformation of Italy due to half a century of urbanization. *Land Use Policy*, *67*, 387-400.

Rosenfeld, A. H., Akbari, H., Bretz, S., Fishman, B. L., Kurn, D. M., Sailor, D., & Taha, H. (1995). Mitigation of urban heat islands: Materials, utility programs, updates. *Energy and Buildings*, *22*(3), 255-265.

Sailor, D. J. (2008). A green roof model for building energy simulation programs. *Energy and Buildings*, *40*(8), 1466-1478.

Salata, F., Golasi, I., Lieto Vollaro A., & Lieto Vollar, R. (2015). How high albedo and traditional buildings' materials and vegetation affect the quality of urban microclimate. A case study. *Energy and Buildings*, *99*, 32-49.

Song, J., Du, S., Feng, X., & Guo, L. (2014). The relationship between landscape compositions and land surface temperature: Quantifying their resolution sensitivity with spatial regression models. *Landscape and Urban Planning, 123*, 145-157.
Tan, Z., Lau, K. K.-L., & Ng, E. (2016). Urban tree design approaches for mitigating daytime urban heat island effects in a high-density urban environment. *Energy and Buildings, 114*, 265-274.
Tayyebi, A., Shafizadeh-Moghadam, H., & Tayyebi, A. H. (2018). Analyzing long-term spatio-temporal patterns of land surface temperature in response to rapid urbanization in the mega-city of Tehran. *Land Use Policy, 71*, 459-469.
Theodosiou, T. G. (2003). Summer period analysis of the performance of a planted roof as a passive cooling technique. *Energy and Buildings*, *35*(9), 909-917.
Tong, H., Walton, A., Sang, J., & Chan, J.C. (2005). Numerical simulation of the urban boundary layer over the complex terrain of Hong Kong. *Atmospheric Environment, 39*(19), 3549-3563.
United Nations, Department of Economic and Social Affairs. (2009). *World Urbanization Prospects: The 2009 Revision*. Retrieved January 7, 2019 from http://wedocs.unep.org/bitstream/handle/20.500.11822/18401/World_Urbanization_prospects_2009_Revision.pdf?sequence=1&isAllowed=y
United Nations, Department of Economic and Social Affairs. (2018). *2018 Revision of World Urbanization Prospects*. Retrieved May 19, 2019 from https://www.un.org/development/desa/publications/2018-revision-of-world-urbanization-prospects.html
United States Census Bureau. (2015). *2010 Census Gazetteer Files. Urban Areas*. Retrieved January 7, 2019 from https://www.census.gov/geo/maps-data/data/gazetteer2010.html
United States Census Bureau, Population Division. (2018). *Annual Estimates of the Resident Population for Incorporated Places of 50,000 or More, Ranked by July 1, 2017 Population: April 1, 2010 to July 1, 2017*. Retrieved January 7, 2019 from https://factfinder.census.gov/faces/tableservices/jsf/pages/productview.xhtml?src=bkmk.
U.S. climate data. (2019). *Weather averages*. Retrieved January 7, 2019 from https://www.usclimatedata.com/climate/united-states/us
Wan, Z., Zhang, Y., Zhang, Q., & Li, Z. (2002) Validation of the land-surface temperature products retrieved from Terra Moderate Resolution Imaging Spectroradiometer data. *Remote Sensing of Environment*, *83*(1-2), 163-180.
Wang, C., Myint, S. W., Wang, Z., & Song, J. (2016). Spatio-temporal modeling of the urban heat island in the Phoenix metropolitan area: Land use change implications. *Remote Sensing*, *8*(3), 185.
Wang, C., Myint, S. W., Fan, P., Stuhlmacher, M., & Yang, J. (2018). The impact of urban expansion on the regional environment in Myanmar: A case study of two capital cities. *Landscape Ecology*, *33*(5), 765-782.
Wentz, E. A., York, A. M., Alberti, M., Conrow, L., Fischer, H., Inostroza, L., Jantz, C., Pickett, S.T.A., Seto, K. C., & Taubenböck, H. (2018). Six fundamental aspects for conceptualizing multidimensional urban form: A spatial mapping perspective. *Landscape and Urban Planning*, *179*, 55-62.
Wickham, J., Stehman, S. V., Gass, L., Dewitz, J. A., Sorenson, D. G., Granneman, B. J., Gass, L., Dewitz, J. A., Sorenson, D. G., Granneman, B. J., Poss, R.V., & Baer, L. A. (2017).

Thematic accuracy assessment of the 2011 national land cover database (NLCD). *Remote Sensing of Environment*, *191*, 328-341.

Worldwatch Institute (2013). State of the World 2007: Our Urban Future. New York, New York: W.W. Norton & Company, Inc.

Yang, J., & Wang, Z.-H. (2017). Planning for a sustainable desert city: The potential water buffering capacity of urban green infrastructure. *Landscape and Urban Planning, 167*, 339-347.

Yang, J., Wang, Z.-H., Kaloush, K. E., & Dylla, H. (2016). Effect of pavement thermal properties on mitigating urban heat islands: A multi-scale modeling case study in Phoenix. *Building and Environment, 108*, 110-121.

Yang, L., Huang, C., Homer, C. G., Wylie, B. K., & Coan. M. J. (2003). An approach for mapping large-area impervious surfaces: Synergistic use of Landsat 7 ETM+ and high spatial resolution imagery. *Canadian Journal of Remote Sensing, 29*(2), 230-240.

Yokohari, M., Brown, R. D., Kato, Y., & Moriyama, H. (1997). Effects of paddy fields on summertime air and surface temperatures in urban fringe areas of Tokyo, Japan. *Landscape and Urban Planning, 38*(1-2), 1-11.

Yu, C., & Hien, W. N. (2006). Thermal benefits of city parks. *Energy and Buildings, 38*(2), 105-120.

Yuan, F., & Bauer, M. E. (2007). Comparison of impervious surface area and normalized difference vegetation index as indicators of surface urban heat island effects in Landsat imagery. *Remote Sensing of Environment, 106*(3), 375-386.

Yue, W., & Xu, L. (2013). Thermal environment effect of urban water landscape. *Shengtai Xuebao/Acta Ecologica Sinica, 33*(6), 1852-1859.

Zhang, P., Imhoff, M.L., Wolfe, R.E., & Bounoua, L. (2010) Characterizing urban heat islands of global settlements using MODIS and nighttime lights products. *Canadian Journal of Remote Sensing, 36*(3), 185–196

Zhang, X., Zhong, T., Feng, X., & et al. (2009). Estimation of the relationship between vegetation patches and urban land surface temperature with remote sensing. *International Journal of Remote Sensing, 30*, 2105-2118.

Zhang, Y., Murray, A. T., & Turner, B. L. (2017). Optimizing green space locations to reduce daytime and nighttime urban heat island effects in Phoenix, Arizona. *Landscape and Urban Planning, 165*, 162-171.

Zhao, L., Lee, X., Smith, R. B., & Oleson, K. (2014). Strong contributions of local background climate to urban heat islands. *Nature, 511*(7508), 216.

Zhao, Q., Myint, S. W., Wentz, E. A., & Fan, C. (2015). Rooftop Surface Temperature Analysis in an Urban Residential Environment. *Remote Sensing*, *7*(9), 12135–12159.

Zhao, Q., Sailor, D. J., & Wentz, E. A. (2018). Impact of tree locations and arrangements on outdoor microclimates and human thermal comfort in an urban residential environment. *Urban Forestry & Urban Greening*, *32*, 81-91.

Zheng, B., Myint, S. W., & Fan, C. (2014). Spatial configuration of anthropogenic land cover impacts on urban warming. *Landscape and Urban Planning, 130*, 104-111.

Zhou, W., Huang, G., & Cadenasso, M. L. (2011). Does spatial configuration matter? Understanding the effects of land cover pattern on land surface temperature in urban landscapes. *Landscape and Urban Planning, 102*(1), 54-63.

Zhou, .D, Zhao, S., Liu, S., Zhang, L., & Zhu, C. (2014) Surface urban heat island in China's 32 major cities: spatial patterns and drivers. *Remote Sensing of Environment, 152*, 51-61.

Zullo, F., Fazio, G., Romano, B., Marucci, A., & Fiorini, L. (2019). Effects of urban growth spatial pattern (UGSP) on the land surface temperature (LST): A study in the Po Valley (Italy). *Science of The Total Environment, 650*, 1740-1751.